Building Engineering 2025, 3(2), 1946.
https://doi.org/10.59400/be1946

Article

Multivariate optimization of mechanically ventilated photovoltaic double-skin façade system for the cold conditions of composite climate zone

Sajan Preet[1,2,*], Sanjay Mathur[2], Jyotirmay Mathur[2], Stefan Thor Smith[1], Himanshu Saini[2]

[1] School of Built Environment, University of Reading, Reading RG6 6UR, United Kingdom
[2] Centre for Energy and Environment, Malaviya National Institute of Technology, Jaipur 302017, India
*** Corresponding author:** Sajan Preet, s.preet@reading.ac.uk

CITATION

Preet S, Mathur S, Mathur J, et al. Multivariate optimization of mechanically ventilated photovoltaic double-skin façade system for the cold conditions of composite climate zone. Building Engineering. 2025; 3(2): 1946. https://doi.org/10.59400/be1946

ARTICLE INFO

Received: 28 October 2024
Accepted: 25 December 2024
Available online: 1 April 2025

Abstract: Assessing the performance of a multi-storey building equipped with a mechanically ventilated photovoltaic-double skin façade (photovoltaic-DSF) system during cold weather conditions is crucial. This is because the demand for heating in buildings rises as outdoor temperatures decrease. This study formulates and verifies mathematical models to evaluate the energy performance of a building integrated with a mechanically ventilated photovoltaic-double skin façade (photovoltaic-DSF) system in Jaipur's cold climate, which is part of India's composite climate zone. The system was installed and observed during the winter months (December to February). The experimental design utilised a Taguchi L25 orthogonal array, considering variables such as air cavity thickness, air velocity, and photovoltaic (PV) panel transparency. Based on experimental findings, multiple linear regression analysis was used to predict three key performance metrics: The solar heat gain coefficient (SHGC), photovoltaic panel electrical output, and indoor daylight illuminance, all as influenced by the design parameters. The analysis of variance (ANOVA) confirmed the statistical significance of these relationships, and the model demonstrated a strong correlation with field measurements (R^2 > 0.90), validating the accuracy of the developed mathematical correlations. The analysis reveals that a photovoltaic DSF system integrated into a multi-storey building, featuring a photovoltaic panel with 50% transparency, an air velocity of 5 m/s, and a 50 mm air cavity, achieves maximum energy performance under cold climate conditions in a composite climate. These insights can help in designing energy-efficient photovoltaic-DSF systems specifically optimised for winter conditions in composite climate zones.

Keywords: double-skin façade; regression analysis; mechanical ventilation; multivariate optimization; ANOVA analysis

1. Introduction

In the current scenario, nearly 30% of the world's energy is consumed by commercial and residential buildings. This figure is expected to rise to 50% by the end of 2030. The increase in energy consumption is attributed to significant growth in the construction sector [1]. Given these projections, countries around the world are increasingly acknowledging the significance of energy-efficient building designs. The United Kingdom has required net-zero energy buildings under its Energy Performance of Buildings Directive [2]. In the United States, government-led initiatives like LEED (Leadership in Energy and Environmental Design) and the Energy Star programme have been introduced to lower building energy consumption [3]. Buildings in India must now adhere to the Energy Conservation Building Code [4]. The building layout is optimised through passive design elements to maximise thermal and visual comfort and minimise energy usage [5,6]. Compared to single-envelope designs, double-skin

façades (DSFs) have become popular passive heating and cooling solutions due to their lower energy demands [7].

Double skin façades (DSFs) effectively balance energy savings with occupant comfort, both in terms of thermal and visual aspects. Semi-transparent photovoltaic (PV) modules installed on the exterior of a DSF provide aesthetic appeal and generate on-site energy. Additionally, they help maintain optimal daylight levels and reduce indoor glare [8,9]. In the past decade, double-skin façades (DSFs) have garnered significant attention from researchers due to their low U-value properties and ability to enhance heat gain in built environments by utilizing inner circulation airflow strategies [10–13]. Naturally ventilated systems have demonstrated superior performance compared to dual-glazing window systems, especially in terms of transferring heat from the cavity to indoor spaces [14,15]. However, the energy performance enhancements in photovoltaic-DSF systems with natural ventilation are constrained, primarily because of the low convective heat transfer rate between the envelope and the cavity [16,17].

Consequently, researchers have increasingly turned their attention to mechanically ventilated DSF systems to enhance convective heat transfer within the air cavity [18,19]. In these systems, crucial parameters—such as the transparency of photovoltaic modules, air cavity thickness, and ventilation rate—are vital for optimising energy savings [20–22]. The current research aims to conduct a comprehensive sensitivity analysis on various parameters to optimise the energy performance of mechanically ventilated double-skin façade (DSF) systems under winter conditions in a composite climate. Initially, a Taguchi analysis was performed to streamline the set of experiments. The influence of geometric design parameters was evaluated using the signal-to-noise (S/N) ratio. Subsequently, mathematical correlations were developed through multiple linear regression analysis, and their significance was rigorously verified using analysis of variance (ANOVA). The experimental validity of these mathematical correlations was further confirmed through a series of confirmation tests, as detailed in this research article.

2. Literature review

2.1. Studies on the transparency of outer skin

Lu and Law [10] found that integrating semi-transparent photovoltaic windows with conventional windows reduced heating loads by 23%, enhancing energy efficiency during colder seasons. However, Miyazaki et al. [11] observed that while increasing PV panel transparency reduced the need for heating and lighting, it also raised cooling loads in warmer conditions. This finding highlights a trade-off between winter and summer performance. Peng et al. [23] found that photovoltaic double-glazing uses approximately half the energy of traditional double-glazing. Wang et al. [12] demonstrated that dual-glazed photovoltaic windows achieved energy savings of 25.3% and 10.7% compared to transparent and low-emissivity windows, respectively. Chen et al. [13] determined that a dual-glazed photovoltaic window with a 0.87 coverage ratio was the most effective for energy savings. Wang et al. [14] also showed that higher PV coverage ratios resulted in greater energy savings during the summer, emphasising the seasonal advantages. Wang et al. [24] discovered that a naturally

ventilated DSF system with internal double glazing in the Yangtze River area achieved 45.5% energy savings compared to standard double-glazed units, demonstrating its potential for enhancing energy efficiency in buildings. Srisamranrungruang and Hiyama [25] demonstrated that incorporating a perforated sheet with a 50% perforation ratio in DSFs reduced glare by 40% and optimised energy savings, effectively balancing efficiency with visual comfort. Sharma et al. [26] found that incorporating perforated metallic sheets into DSFs reduced the Solar Heat Gain Coefficient (SHGC) by 14.7%, thereby improving thermal performance. Zhang et al. [27] showed that incorporating a bio-productive layer in naturally ventilated double skin façades enhances daylighting and mitigates winter glare risks.

2.2. Studies on the ventilation modes

Han et al. [28] discovered that photovoltaic-double skin façade systems significantly enhance energy efficiency in winter by transferring the heat captured within the cavity to indoor spaces, thereby improving energy savings in colder climates. Peng et al. [29] concluded that natural ventilation significantly reduced heating loads in buildings with photovoltaic-double skin façade systems by utilising passive airflow and heat transfer. In a subsequent study, Peng et al. [23] compared various operational modes of photovoltaic-DSF systems, revealing that naturally ventilated configurations had a lower Solar Heat Gain Coefficient (SHGC) for solar heat control, whereas non-ventilated systems provided better insulation due to a lower U-value. Wang et al. [12] confirmed that photovoltaic double-glazing, combined with natural ventilation, was the most energy-efficient solution in Hong Kong, demonstrating its potential effectiveness in various climates. Inan and Basaran [30] compared buoyancy and mechanical ventilation for transparent glass-based double skin façade systems, finding that mechanical ventilation used less energy for heating, making it more efficient in certain situations. Ioannidis et al. [16] developed a Nusselt number to specifically measure convective heat transfer in photovoltaic double-skin façade systems. Their research showed that mechanically ventilated systems had a significantly higher rate of convective heat transfer compared to naturally ventilated systems. This was supported by experimental results, which indicated a temperature difference of less than 2 °C between the photovoltaic panel and the surrounding air. These findings validate the accuracy of the convective heat transfer predictions and highlight the effectiveness of mechanical ventilation in improving the thermal performance of photovoltaic-DSF systems. Radmard et al. [17] validated their results through simulation, confirming their reliability. Yang et al. [18] found that mechanical ventilation in photovoltaic-DSF systems reduced cooling loads by lowering the Solar Heat Gain Coefficient (SHGC), but naturally ventilated systems achieved greater overall energy savings due to the energy costs associated with mechanical fan operation. Preet et al. [19] conducted a comparative study on the performance of natural versus mechanical ventilation during the hot summer months in a composite climate zone. Their findings indicated that mechanically ventilated double-skin façade (DSF) systems significantly outperformed naturally ventilated systems. The mechanically ventilated systems not only provided better thermal comfort but also achieved greater energy savings, highlighting their superior efficiency in managing

thermal loads in such climates. Pourshab et al. [31] used numerical modelling to show that buoyancy-ventilated DSF systems with horizontal Venetian blinds significantly improved energy efficiency by enhancing convective flow, outperforming vertical blinds. This underscores the role of design elements in boosting thermal performance in DSF systems. Jankovic and Goia [32] used the Design of Experiments (DOE) method to study DSF energy performance, focusing on parameters like solar irradiance, temperature difference, Venetian blind angle, and inlet/outlet cross-sectional area. They found that blind slat angle and solar irradiance had the most significant effects on heat flux, air cavity temperature, airflow rate, and heat loss, highlighting the importance of optimising slat angles and solar geometry for better DSF performance. Jankovic et al. [22] also stressed the need to fully understand the impacts of airflow and solar geometry on glazing properties. Tao et al. [33] showed that increasing louvre size, height, and aspect ratio improved ventilation rates by 14.8%, 15.3%, and 2.9%, respectively, demonstrating the influence of louvre geometry on airflow and thermal dynamics in DSF systems. Lin et al. [34] developed a naturally ventilated DSF with adjustable louvres for China's temperate climate, achieving 12% energy savings compared to conventional DSFs, showcasing the benefits of adaptable shading. Jankovic and Goia [35] suggested that moderate ventilation rates should be used for Venetian blind-based double skin façade systems to optimise their performance throughout the year.

2.3. Studies on the air cavity width

Preet et al. [19] examined the effect of air cavity thickness on the performance of double-skin façade (DSF) systems during the hot summer months in a composite climate zone. Their study found that an air cavity thickness of 200 mm is optimal for achieving maximum energy savings, highlighting the importance of precise design parameters in enhancing DSF efficiency in such climates. Tao et al. [36] discovered that Venetian blinds in photovoltaic-DSF systems significantly impacted performance, with upward louvre angles (30°–67.5°) improving airflow, while low-emitting glazing enhanced the stack effect by 13%. An optimal cavity width was identified as 150–300 mm. Sotelo-Salas et al. [37] determined that a 400 mm air cavity, 25 μm droplet size, and 600 mm nozzle spacing were optimal for DSF performance. Tao et al. [38] also identified a cavity width of 200 mm and height of 300 mm as optimal for maximising energy savings, underscoring the role of geometric design in improving DSF efficiency.

2.4. Research gap and objective

Mechanically ventilated double skin façade (DSF) systems have attracted significant research interest due to their ability to reduce heating loads in built environments. Recent studies have focused on key geometric design parameters and their effects on energy performance. For instance, Yang et al. [18] analysed the influence of photovoltaic panel transparency, air velocity, and air cavity thickness on DSF performance, noting that each factor plays a crucial role in energy efficiency. Jankovic and Goia [32] conducted parametric studies that quantified airflow inside the DSF cavity, examining the impact of solar radiation, Venetian blind angles, and the

cross-sectional areas of the inlet and outlet. These studies highlighted the importance of airflow in optimising DSF systems.

Ioannidis et al. [16] explored the impact of air cavity thickness in cold climates, such as those found in Canada, while Yang et al. [18] examined how roller blinds influenced energy performance at varying cavity thicknesses. Despite these studies, research on mechanically ventilated DSF systems has primarily focused on a limited set of parameters, leaving significant gaps in understanding how variations in photovoltaic (PV) panel transmittance, airflow rates inside the cavity, and cavity thicknesses impact DSF performance, especially under cold conditions in composite climate zones. The interaction among these design elements is complex and multi-dimensional. For example, lower photovoltaic panel transmittance decreases net heat gain to indoor spaces, reducing daylight penetration and outdoor visibility. However, this also enhances the system's energy efficiency by improving the power output of the PV panels. Conversely, increasing air velocity through the cavity can boost the rate of convective heat recovery, improving thermal performance by evacuating heat more effectively from the façade. Yet, this improvement may come at the cost of reduced overall energy savings due to the additional energy consumed by the fans required to maintain airflow. Thus, balancing air cavity thickness, air velocity, and photovoltaic panel transparency is crucial for optimising both thermal and visual comfort within the built environment. This optimisation must ensure energy efficiency without causing excessive demand for mechanical ventilation systems.

In this study, a comprehensive parametric investigation was conducted to assess the influence of three critical design parameters—air cavity thickness, air velocity, and photovoltaic panel transparency—on the performance of mechanically ventilated photovoltaic-DSF systems during the winter in a composite climate zone. The experimental data obtained allowed for the development of mathematical correlations aimed at predicting the optimal combination of these design factors to maximise energy savings. These correlations provide valuable insights into the fine-tuning of mechanically ventilated DSF systems for achieving energy-efficient building envelopes. By leveraging these optimised parameters, commercial-scale DSF-integrated building designs can significantly reduce heating loads, improve thermal and visual comfort, and enhance overall energy performance, making these systems a practical solution for sustainable architecture in composite climates.

3. Experimental setup

In this photovoltaic-DSF module design, a semi-transparent Cadmium Telluride (CdTe) photovoltaic module forms the external skin of the system, while a 6 mm clear glass pane is used as the internal layer. The separation between these two layers is defined by the cavity thickness. **Figure 1a** demonstrates the positioning of the photovoltaic-DSF system externally on the building structure, where the transparency levels of the CdTe PV module are varied to examine their impact on energy efficiency and performance. **Table 1** illustrates details specifying transparency levels of the CdTe photovoltaic module employed in the study, providing a comparative basis for analyzing how different degrees of transparency influence factors such as daylight penetration, solar heat gain, and overall energy performance.

Figures 1b,c depict the detailed design of the photovoltaic window frame in the photovoltaic-DSF system. These frames include inlet and outlet openings for airflow, strategically located at the top and bottom of the system to facilitate effective ventilation. Mechanical ventilation is provided by axial fans installed in the input aperture cavity of the photovoltaic-DSF system, ensuring continuous airflow through the cavity. **Figure 1d** offers an internal view of the system, illustrating the layout and arrangement from the perspective of the photovoltaic-DSF module. The system, measuring 3 m × 3 m × 3 m, facilitates a comprehensive investigation of airflow dynamics, energy savings, and thermal performance under controlled conditions.

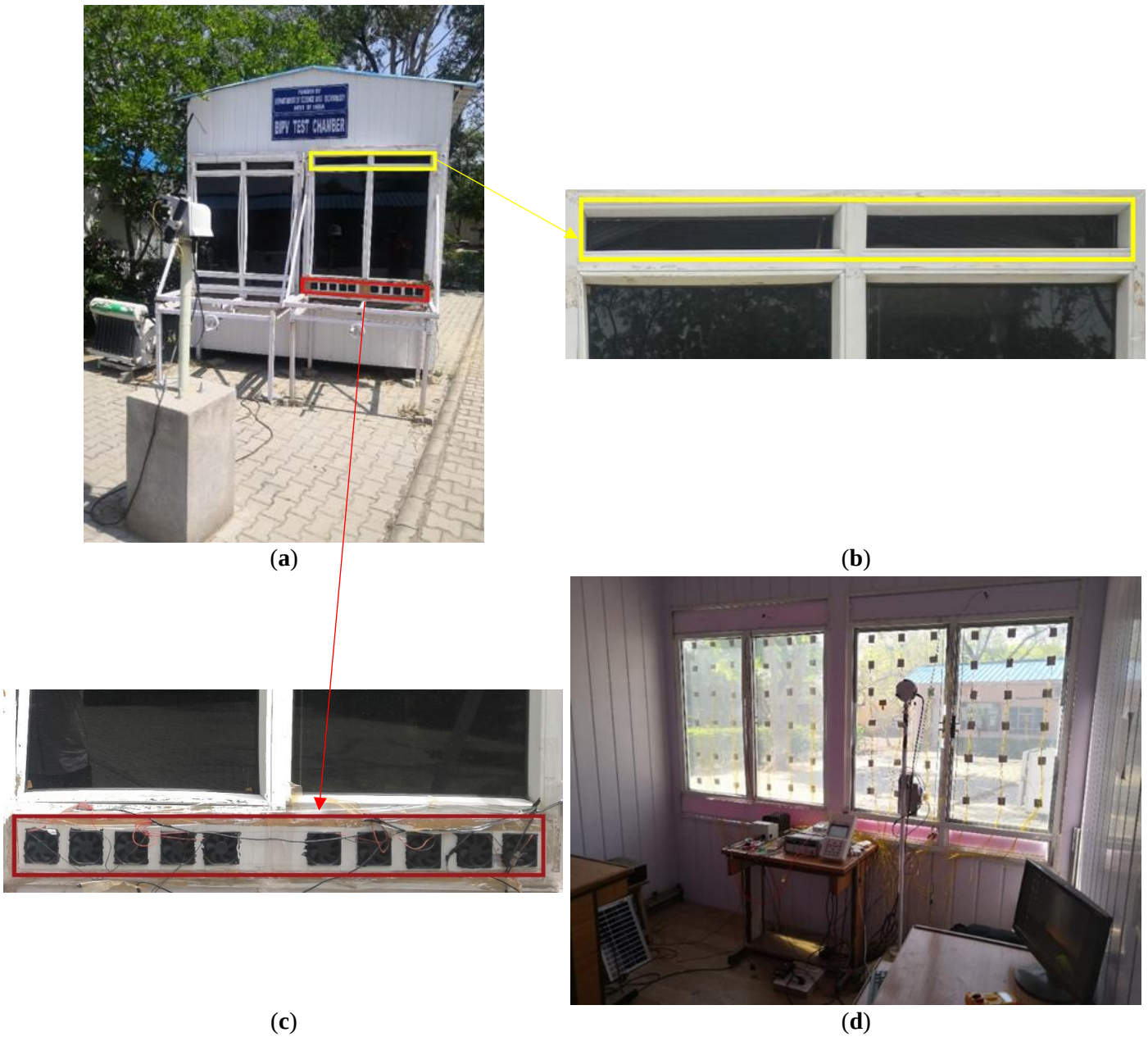

(**a**) (**b**)

(**c**) (**d**)

Figure 1. Pictorial view of experimental setup, **(a)** exterior view of PV-DSF system; **(b)** outlet opening of air cavity; **(c)** position of fans at inlet opening of air cavity; **(d)** interior view of PV-DSF system.

Table 1. Properties of the CdTe PV module at STC (provided by the manufacturer) [39].

Parameters (unit)	**PV1**	**PV2**	**PV3**	**PV4**	**PV5**
Nominal power [Pm] (W)	71.34	63.5	55.68	47.85	43.50
Short circuit current [I_{sc}] (A)	0.880	0.780	0.680	0.590	0.540
Open circuit voltage [V_{oc}] (V)	116.0	116.0	116.0	116.0	116.0
Current at maximum power point [I_{mp}] (A)	0.820	0.730	0.640	0.550	0.500
Voltage at maximum power point [V_{mp}] (V)	87.00	87.00	87.00	87.00	87.00
Efficiency [η] (%)	9.910	8.800	7.730	6.640	6.040
Temperature coefficient of *I*sc (%/°C)	0.060	0.060	0.060	0.060	0.060
Temperature coefficient of *V*oc (%/°C)	−0.321	−0.321	−0.321	−0.321	−0.321
Temperature coefficient of Pm (%/°C)	−0.214	−0.214	−0.214	−0.214	−0.214

This design incorporates forced airflow to optimize convective heat transfer, particularly enhancing the system's thermal performance in the winter season of composite climate zones. The axial fans play a crucial role in modulating the airflow within the cavity, directly impacting the performance of overall system.

The U-values of the walls and roof in this photovoltaic-DSF module design are maintained at 0.493 W/m²K for the walls and 0.352 W/m²K for the roof. These values comply with the Energy Conservation Building Code (ECBC) guidelines for India's composite climate. as detailed by Saxena and Das [4]. This ensures that the building envelope has appropriate insulation to minimize heat transfer, thereby enhancing energy efficiency. A key feature of the system is its movable air cavity, which allows for the adjustment of the cavity thickness. This flexibility is made possible through a photovoltaic module integrated window that is mounted on rollers. The window can move along a groove via a screw system, allowing for easy adjustments to the cavity thickness. The adjustable sides of the cavity are insulated with high thermal resistance material, enhancing the system's thermal performance by minimising unwanted heat losses. This movable air cavity design enhances the adaptability of the system, enabling optimal control over airflow and cavity size to improve energy efficiency and comfort during different climate conditions.

A series of experiments were conducted during the winter season (December to February) of 2020 to evaluate the performance of the photovoltaic double-skin façade (DSF) system in the composite climate of Jaipur, India. Each set of experiments, covering a different range of design parameters as shown in **Table 2** was performed in triplicate. This approach ensured consistent environmental conditions and enhanced the accuracy of the experimental results. For each experiment, the system's output variables, including the solar heat gain coefficient (SHGC), power output of the photovoltaic (PV) panels, and daylight illuminance in the indoor space, were recorded at 15-min intervals. The average value of each response was used for further analysis, ensuring reliability and accuracy in the data. The instruments used in the experimental investigation are detailed in **Table 3**.

India's climate is categorised into five distinct zones, as outlined by Bansal and Minke [40], with Jaipur falling into the composite climate zone. During the winter

season in Jaipur, ambient temperatures typically range between 12 °C and 15 °C [41], representing a cool period in this climate, as shown in **Figure 2**.

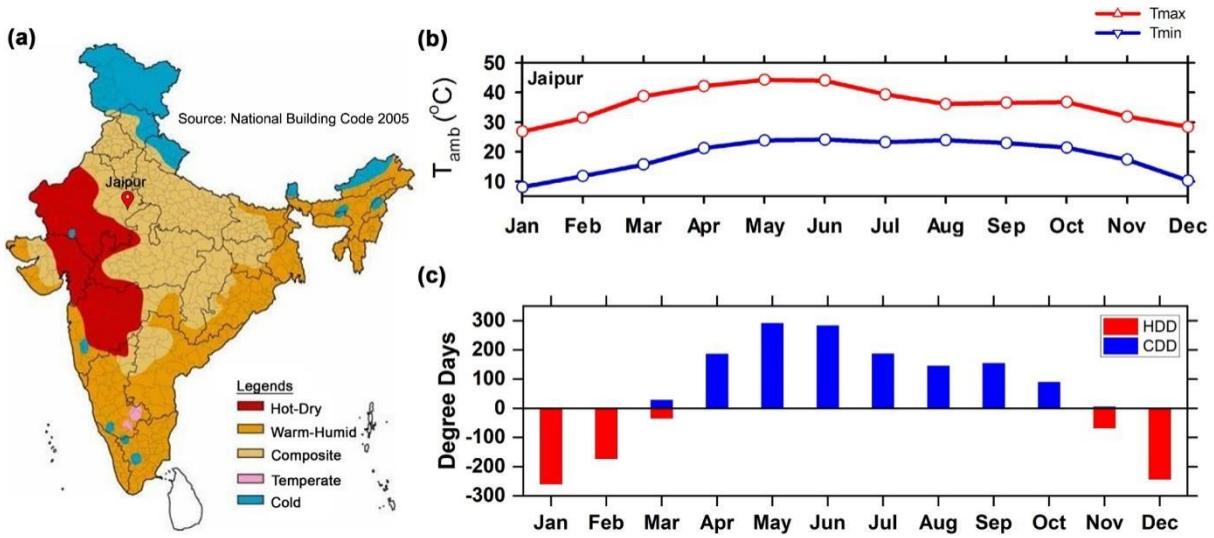

Figure 2. (**a**) Map showing climatic zones of India (BIS, 2016) and location of Jaipur; (**b**) monthly average and of Jaipur; (**c**) heating and cooling degree days for Jaipur [42].

Figure 3 illustrates the incident solar radiation on a vertical plane and the ambient temperature during a typical winter day. The photovoltaic-DSF system successfully maintains the indoor temperature of the constructed space at 21 °C, which aligns well with thermal comfort standards. According to Kumar et al. [43], the mean comfort temperature during the summer season in India's composite climate ranges between 19 °C ± 1 °C and 25 °C ± 1 °C, making the maintained indoor temperature of 21 °C comfortably within this range. This underscores the system's effectiveness in maintaining an optimal thermal environment even in colder winter conditions.

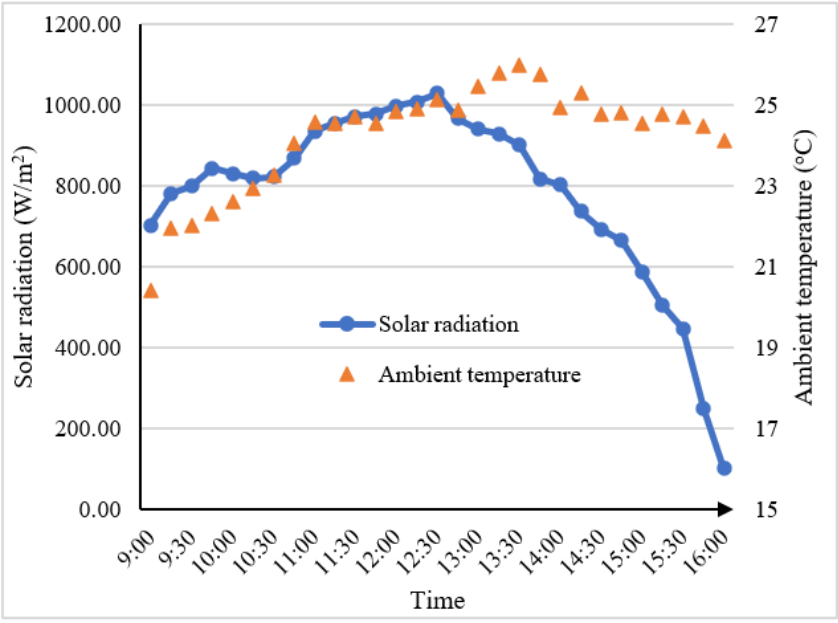

Figure 3. Solar radiation and ambient temperature in winter.

Instrumentation details

The research facility is fully equipped to continuously monitor the environmental and system-specific parameters essential for evaluating the performance of the photovoltaic-DSF system. A weather station by Virtual Instruments is used to track ambient conditions, providing real-time data on external environmental factors that may influence the system's performance.

Key instruments include:

Razon+ Pyrheliometer: Measures both the direct and diffuse components of solar irradiation throughout the day, ensuring accurate solar input data.

Pyranometer: Records the solar radiation transmitted into the interior built space through the photovoltaic-DSF system, offering insight into the system's ability to control sunlight entry.

Convective and Radiative Heat Flux Measurements: These techniques are employed to assess the net heat transfer across the DSF system, following established standards [19,44,45].

L-19 Data Acquisition System: Logs all collected data for later analysis, ensuring accurate tracking of all variables involved in system performance.

To evaluate the electrical performance of the photovoltaic module, an I-V curve tracer manufactured by MECO Instruments is used. This device characterizes the photovoltaic panel's electrical behavior by measuring its current-voltage relationship. For the interior environment, a Testo 480 lux meter is utilized to measure daylight illuminance levels within the room. The lux meter is positioned 1 m away from the PV-DSF window at a height of 0.8 m above the floor, ensuring consistent and reliable readings of indoor lighting conditions [46,47]. **Figure 4** provides a schematic layout of the entire experimental setup, detailing the positions and configurations of all instruments. The specifications of these instruments, along with their roles, are provided in **Table 3**, outlining the precise technical details essential for accurate data acquisition and analysis of the photovoltaic-DSF system's performance.

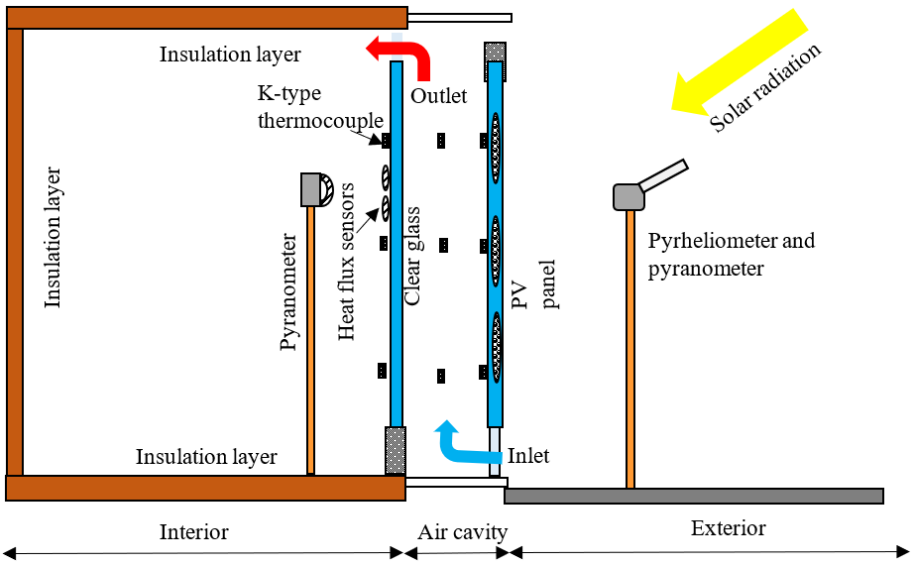

Figure 4. Schematic diagram of PV-DSF system with location of sensors and instruments.

Table 2. Orthogonal array for L25 Taguchi design for winter.

Experiment No.	Operating parameters			Responses		
	Air cavity width (mm)	Air velocity (m/sec)	PV panel transparency (%)	SHGC	Power of PV panel	Lux Level
1	50	2.00	10	0.171	12.91	237
2	50	2.75	20	0.19	12.98	356
3	50	3.50	30	0.2	12	447
4	50	4.25	40	0.212	11.69	578
5	50	5.00	50	0.22	11.49	688
6	100	2.00	20	0.181	13.01	330
7	100	2.75	30	0.21	11.84	418
8	100	3.50	40	0.2	11.72	559
9	100	4.25	50	0.212	11.5	667
10	100	5.00	10	0.141	13.67	248
11	150	2.00	30	0.21	11.98	400
12	150	2.75	40	0.19	11.87	541
13	150	3.50	50	0.2	11.64	632
14	150	4.25	10	0.151	13.78	231
15	150	5.00	20	0.16	13.7	306
16	200	2.00	40	0.194	12	514
17	200	2.75	50	0.203	11.6	609
18	200	3.50	10	0.153	13.81	210
19	200	4.25	20	0.164	13.76	293
20	200	5.00	30	0.173	13	370
21	250	2.00	50	0.199	11.66	580
22	250	2.75	10	0.159	13.75	189
23	250	3.50	20	0.169	13.66	279
24	250	4.25	30	0.17	12.89	358
25	250	5.00	40	0.178	12.55	483

Table 3. List of instruments.

Instrument	Purpose	Manufacturer and model	Specification
Weather Station	Measure ambient temperature, wind velocity	Virtual instrumentation	Wind speed: 0.1 m/s; Wind direction: 1°; Temperature: 0.1 °C
Pyrheliometer and Pyranometer	Measure direct and diffuse radiation incident on PV panel	Kipp and Zonen, Razon+	Response time: 0.2 s Point accuracy: 0.2° Spectral range: 310 nm to 2700 nm Measuring range: 0 to 1500 W/m^2 Data logging: 1 min average
Pyranometer	Measure the solar radiation penetrating through window	Delta-T devices/sunshine SPN1	Sensitivity: 1mV = 1 W.m^{-2} Response time: 100 ms
I-V curve analyzer	Measure electrical performance of PV panel	MECO I-V curve analyser, 9018BT	Measuring range: Max. solar system power: 1000 V, 12 A.
Conductive heat flux sensors	Measure conductive heat flux ingress into indoor spacing	Captec Enterprise	Sensitivity: 2.5 μV/(W/m^2); Response time: 0.3 s

Table 3. (*Continued*).

Instrument	Purpose	Manufacturer and model	Specification
Radiative heat flux sensors	Radiative heat flux ingress into indoor spacing	Captec Enterprise	Sensitivity: 2.5 μV/(W/m^2); Response time: 0.3 s
Hot wire anemometer	Measure the speed of air in natural and mechanical ventilation mode	Extech/SDL350	Range: 0.2 to 25 m/s; Accuracy: ±0.05 m/s; Resolution: 0.01 m/s
Lux meter	Measure the lux level in the built space	Testo 480	Measuring range: 0 to 100000 Lux Resolution: 1 Lux
Datalogger	Log the temperature data measured by thermocouples	KEYSIGHT/34972A LXI	Accepts voltage (20 mV–50 V), temperature and humidity
Power analyzer	Measure the electrical power consumed by fans	Fluke 434-II Energy Analyzer	Measurement Range: 1 V to 1000 V phase to neutral Resolution: 0.1 V Accuracy: ±0.1% of nominal voltage

4. Methodology

This study aims to develop analytical mathematical models to assess the impact of varying design parameters on key performance metrics of a mechanical ventilated Photovoltaic-Double Skin Façade (PV-DSF) system. The models focus on quantifying relationships between the design variables and three critical performance indicators:

- Solar Heat Gain Coefficient (SHGC): A measure of the net heat transfer to the indoor area of the building, affecting the thermal performance of the structure.
- Electrical Power Output: The electricity generated by the integrated photovoltaic panel, which depends on factors such as panel transparency and incident solar radiation.
- Indoor Daylight Illuminance Levels: The amount of natural light transmitted into the interior spaces, critical for maintaining visual comfort and reducing artificial lighting needs.

These mathematical correlations play a crucial role in optimizing the energy performance of building envelope designs, particularly in regions with composite climates like Jaipur, where the system needs to balance thermal comfort and energy efficiency during different seasons.

The research methodology adopted to develop these models is detailed in **Figure 5**, which provides a comprehensive framework for the experimental process, mathematical derivation, and model validation stages. The methodology encompasses:

- Data Collection: Capturing real-time performance data from the PV-DSF system using the described experimental setup.
- Model Development: Formulating equations that describe the behavior of SHGC, electrical power output, and daylight levels based on variations in design parameters such as cavity thickness, air velocity, and panel transparency.
- Validation and Optimization: Testing the accuracy of these models through experimental validation and adjusting the models to find the optimal combination of parameters for maximum energy savings and improved building performance in the cold climate of composite regions.

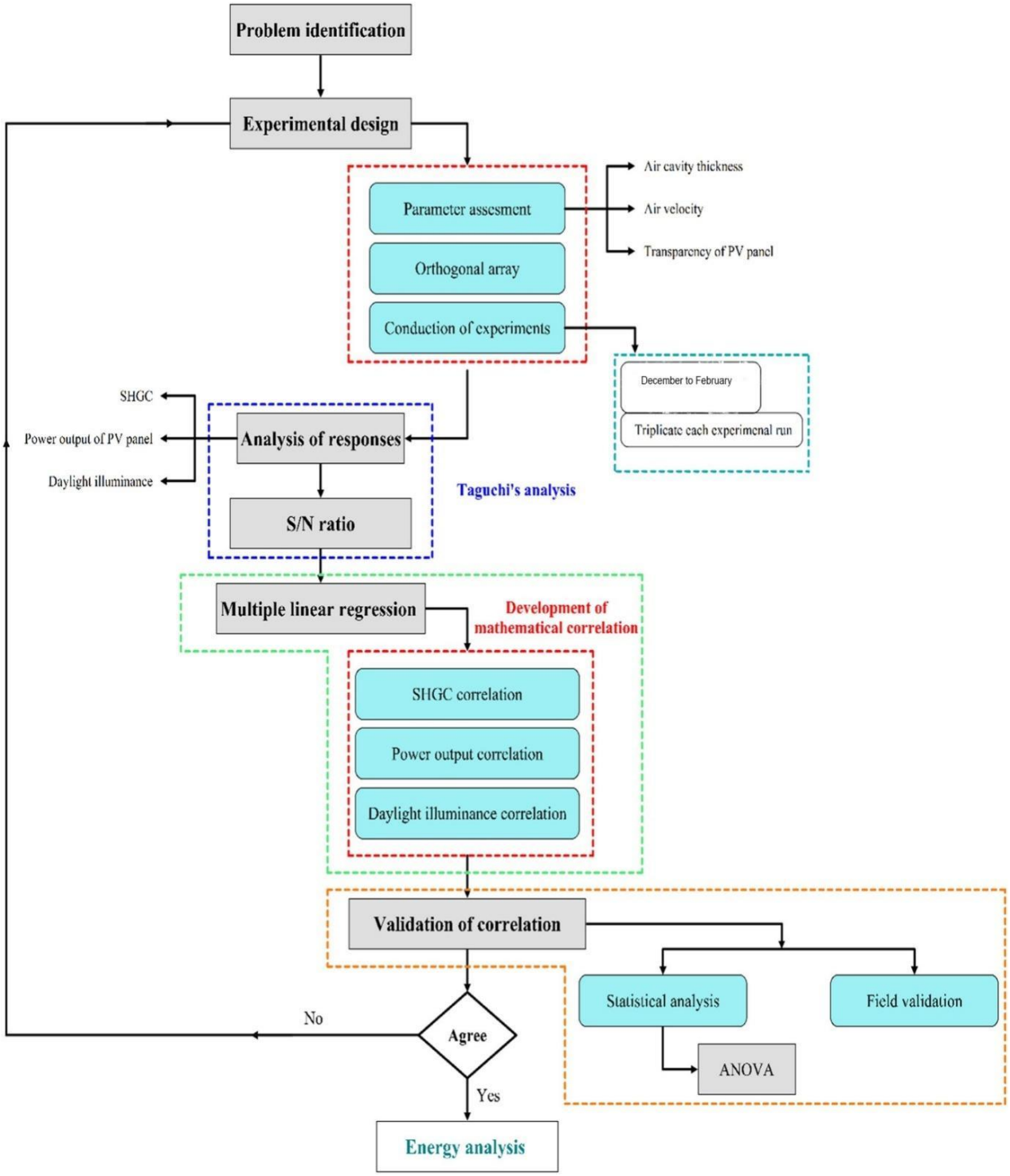

Figure 5. Methodology flow chart for the present study.

4.1. Problem formulation

The energy efficiency of a Photovoltaic-Double Skin Façade (PV-DSF) system in cold climates is largely determined by the consumption of heating systems for indoor spaces, the energy required for lighting, and the power generated by the photovoltaic panel. To achieve maximum energy savings in winter, it is crucial to optimize heat transfer into the building while also enhancing the photovoltaic output and ensuring sufficient natural light indoors. This study focuses on refining the design

parameters of a DSF-integrated building to maximize solar heat gain, improve indoor daylighting, and increase the electrical output of the photovoltaic panel, as outlined in Equation (1).

$$\begin{aligned} Maximum\ SHGC &= f_a(air\ cavity) + f_b(air\ velocity) + f_c(transparency\ of\ PV\ panel) \\ Maximum\ Power &= f_a(air\ cavity) + f_b(air\ velocity) + f_c(transparency\ of\ PV\ panel) \\ Maximum\ daylight\ illu\,min\,a\,nce &= f_a(air\ cavity) + f_b(air\ velocity) + f_c(transparency\ of\ PV\ panel) \end{aligned} \quad (1)$$

f_a, f_b, f_c are the weight of design parameters.

In this study, the Solar Heat Gain Coefficient (SHGC) is determined using the approach recommended by the National Fenestration Rating Council [40], along with methodologies described by Preet et al. [19], Peng et al. [23], and Sharma et al. [26]. The experimental procedure for calculating the solar heat gain coefficient is outlined as follows:

$$SHGC = \frac{G_1 + G_2 + G_3}{G_4} \quad (2)$$

In the experimental configuration, G_1 and G_2 denote the convective and radiative heat flux components, respectively, that pass through the window into the interior space being occupied. G_3 indicates the amount of solar radiation that reaches the occupied area, whereas G_4 represents the total incident solar radiation on the entire PV-DSF system. The solar radiation incident on the vertical facade is computed using the mathematical relationships established by S.P. Sukhatme [48] for estimating solar radiation on tilted surfaces.

4.2. Taguchi design method

Researchers have employed various techniques to address challenges in experimental designs involving multiple variables. Key approaches include Response Surface Methodology (RSM), artificial neural networks (ANN), and the Taguchi method. RSM integrates statistical and mathematical tools to iteratively optimize design parameters, frequently used in reliability analysis [49]. ANN, a machine learning technique, excels at modeling input-output relationships in complex non-linear systems, efficiently handling noisy or incomplete data and allowing rapid updates with new information [50]. Meanwhile, the Taguchi method focuses on process and product optimization, delivering high-quality outcomes with minimal cost. Its strength lies in evaluating multiple variables using fewer experiments, saving both time and resources [51,52]. In this approach, input variables are systematically modified to evaluate their effects on the resulting outcomes [53].

The Taguchi method is recognized as an efficient approach for experimental design, enabling the evaluation of multiple independent variables while minimizing the number of trials required [53]. This method combines statistical and mathematical tools to optimize critical design parameters, enhancing system performance while reducing variability and improving quality [54]. By applying the Taguchi method, researchers can identify key factors influencing a response and determine their optimal combination [55,56]. As illustrated in **Figure 6**, the process follows a systematic flowchart for optimization. Central to this technique is the use of Orthogonal Arrays

(OA), which provide an efficient structure for analyzing the relationship between a response and multiple design parameters under constrained conditions [57]. These act as fractional factorial designs, ensuring balanced representation of parameter combinations across different levels [53].

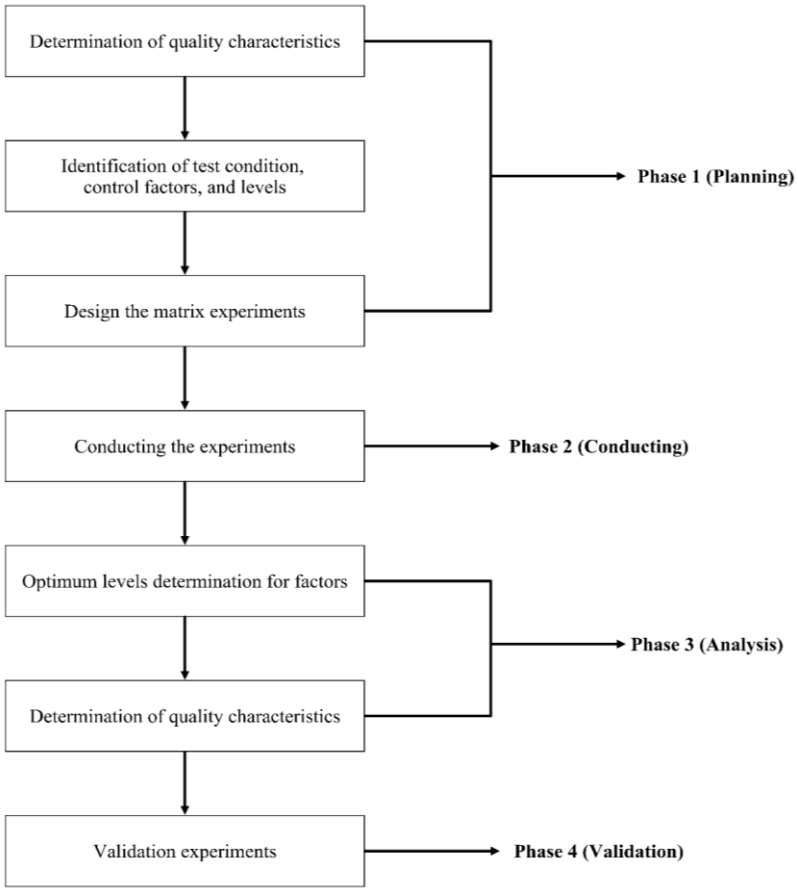

Figure 6. Flowchart representing the Taguchi method.

This study investigates three design parameters, each with five levels. A full factorial design would require 125 experimental runs (5^3), where each combination of parameters is tested. However, by employing the Taguchi method, which uses the degree-of-freedom approach [53], the number of trials is reduced to just 25. This approach significantly decreases the number of experiments while maintaining the statistical reliability of the results, enabling an efficient evaluation of the effects of the different levels of design parameters.

$$N = 1 + \sum_{i=1}^{NV} (L_i - 1) \tag{3}$$

In this study, the total number of trials (N) is determined by the number of independent variables (NV) and the levels of parameters (L). An L25 orthogonal array (OA) was used to structure the experimental design, facilitated by Minitab software (version 15) [47]. The parameter levels were selected based on their anticipated effect on system outputs. A two-level design is employed when the relationship between variables and responses is linear, while more levels (three or more) are used if the

relationship is non-linear [58]. The experiments, based on the L_{25} OA, measured outcomes like the Solar Heat Gain Coefficient (SHGC), photovoltaic power output, and indoor lighting levels, following the Taguchi method. The impact of each parameter on these outcomes was evaluated through signal-to-noise (S/N) ratio analysis, a method that optimizes system performance by distinguishing the desired signal from unwanted variations (noise) [47]. The larger-is-better approach of S/N ratios was used in this study to maximize SHGC, photovoltaic power, and daylight illuminance, aiming to minimize the overall energy demand within the built environment [54,59].

Signal-to-noise ratio (S/N) for larger-the-better is calculated by;

$$\frac{S}{N} = -10\log\left(\frac{1}{n}\sum_{i=1}^{n}\frac{1}{y_i^2}\right) \tag{4}$$

In this study, the "larger-is-better" optimisation principle is applied, where (n) represents the number of experimental trials, and (y_i) is the outcome or response from the ith experiment [60]. A multiple linear regression model is employed to establish mathematical correlations between the design variables and the corresponding performance responses, such as the Solar Heat Gain Coefficient (SHGC), photovoltaic power output, and indoor illuminance levels. These correlations are then validated using analysis of variance (ANOVA), a statistical method that breaks down data variability into different components. ANOVA helps test the significance of the model parameters and ensures that the derived relationships between the variables and responses are statistically robust [61].

Selection of range of parameters

To develop mathematical correlations for estimating key performance metrics—such as the Solar Heat Gain Coefficient (SHGC), photovoltaic power output, and natural daylighting—three primary design parameters were defined: Cavity thickness, air velocity, and photovoltaic panel transparency.

The range for cavity thickness was set between 50 mm and 250 mm. Analytical models indicate that thicknesses below 40 mm cause boundary layer overlap between the two panes, hindering air circulation and leading to heat accumulation [39,62]. Therefore, 50 mm was selected as the minimum size, while past research demonstrated a substantial decrease in heat gain between 50 mm and 200 mm. Beyond 200 mm, the additional benefit diminishes, so the upper limit was set at 250 mm [19].

Air velocities were determined based on initial tests, ranging between 2 m/s and 30 m/s inside the cavity. To maintain energy efficiency by ensuring that fan power consumption remained below the energy generated by the photovoltaic (PV) panels, and to keep noise levels in occupied areas under 55 dB [63], an upper velocity limit of 5 m/s was chosen.

Photovoltaic panel transparency, which influences both power generation and daylighting, was varied between 10% and 50%. A transparency of 10% maximizes power output, while 50% offers better daylight penetration [11]. These design parameter ranges are summarized in **Table 4**.

Table 4. Variation of operating parameters.

Parameters	Symbol	Level 1	Level 2	Level 3	Level 4	Level 5
Air cavity width (mm)	A	50	100	150	200	250
Air velocity (m/s)	B	2.00	2.75	3.50	4.25	5.00
PV panel transparency (%)	C	10	20	30	40	50

5. Results and discussion

5.1. Main effect plot

In this study, main effect plots are employed to illustrate how variations in design parameters influence the key performance metrics of the photovoltaic-DSF system, including the Solar Heat Gain Coefficient (SHGC), the power output of the photovoltaic panels, and the indoor daylight illuminance. In these plots, each parameter's different levels are connected by lines. A horizontal line in a main effect plot suggests that varying the parameter has little to no impact on the response, while a sloped line indicates that changes in the parameter significantly influence the system's performance. These plots help to identify which design parameters most strongly affect the system and guide the optimization of the photovoltaic-DSF configuration.

a) Main effect plot of solar heat gain coefficient (SHGC)

Figure 7a illustrates the main effect plot of the Solar Heat Gain Coefficient (SHGC) for various air cavity thicknesses in the photovoltaic double-skin façade (DSF) system. It can be observed that with variations in air cavity thickness from 50 mm to 250 mm, the SHGC decreased, as indicated by the decline in the signal-to-noise (S/N) ratio. The figure shows a significant variation in the S/N ratio from 50 mm to 200 mm, with minimal variation beyond 200 mm. This indicates that the SHGC dropped significantly from 50 mm to 200 mm, with only minimal reduction thereafter. This behaviour is primarily due to the boundary layer interactions at a 50 mm air cavity thickness, which restrict air movement through the cavity, resulting in a greenhouse effect. At larger air cavity thicknesses, from 200 mm to 250 mm, the increased air mass within the cavity restricts air movement [64]. The convective heat transfer efficiency diminishes due to a lower temperature gradient and decreased turbulence in the larger air volume, limiting the system's ability to remove heat through the cavity. Similar observations have been reported by Peng et al. [23], Peng et al. [65] and Preet et al. [39].

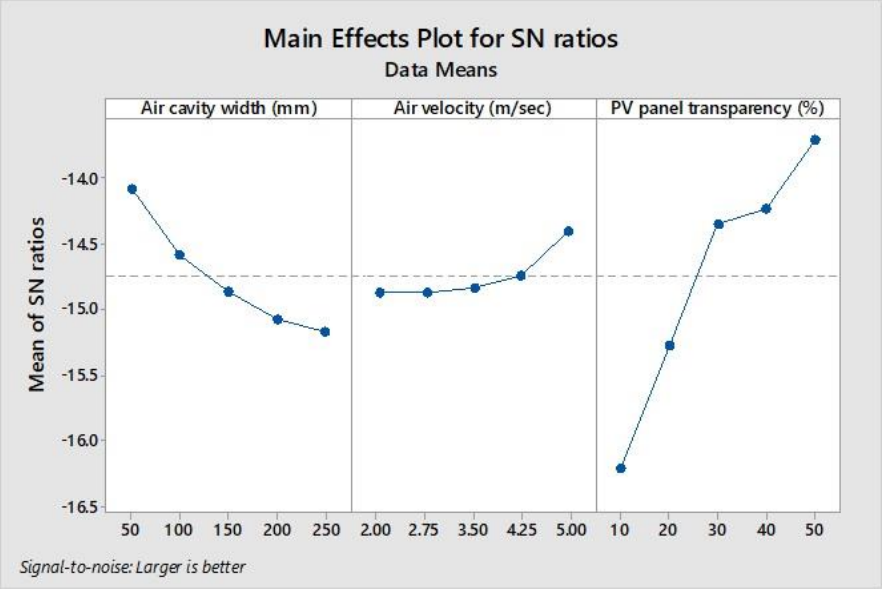

Figure 7. Impact of air cavity, air velocity, and transparency of PV panel on SHGC.

Figure 7b illustrates that as air velocity within the cavity increases, the Solar Heat Gain Coefficient (SHGC) also rises, indicated by the upward trend in the signal-to-noise (S/N) ratio. This increase is due to enhanced convective heat transfer from both the photovoltaic (PV) panel and the inner pane, leading to more heat being transferred into the interior space. The higher air velocity facilitates the movement of heated air, resulting in a greater net heat flow from the cavity to the indoor environment, thereby increasing solar heat gain within the building. These findings align with the results reported by Mateus et al. [66], Ioannidis et al. [67], and Yang et al. [18], which also observed that higher air velocities within DSF systems improve convective heat transfer and solar heat gain.

Figure 7c highlights the impact of varying photovoltaic panel transparency levels on the Solar Heat Gain Coefficient (SHGC). As the transparency of the photovoltaic panel increases, the SHGC significantly rises, which is reflected by a increase in the signal-to-noise (S/N) ratio. This trend is primarily due to the reduction in the area occupied by photovoltaic cells, allowing more direct sunlight to penetrate through the PV panel. Similar results were observed by Miyazaki et al. [11], confirming that increased transparency leads to higher solar heat gain due to greater sunlight transmission.

b) Main effect plot of the electrical output of PHOTOVOLTAIC panel

Figure 8a demonstrates the impact of air cavity thickness on the electrical output of the photovoltaic (PV) panel. As the cavity thickness increases, there is a notable rise in the panel's electrical output, indicated by an increase in the signal-to-noise (S/N) ratio. At a 50 mm air cavity width, the overlapping boundary layers restrict air movement inside the cavity, resulting in low convective heat loss from the PV panel to the air within the cavity, and consequently, lower power output. However, as the air cavity thickness increases from 50 mm to 200 mm, the convective heat loss from the PV panel to the air inside the cavity is enhanced, leading to an improvement in the panel's power output. Beyond 200 mm, the increased air mass within the cavity

restricts turbulence, thereby reducing convective heat loss from the PV panel to the air inside the cavity. The most significant gains in power output are observed between 50 mm and 200 mm of cavity thickness, with diminishing returns beyond 200 mm. This suggests that the optimal cavity thickness for maximizing electrical output lies within this range. Similar observation have been reported by Preet et al. [19].

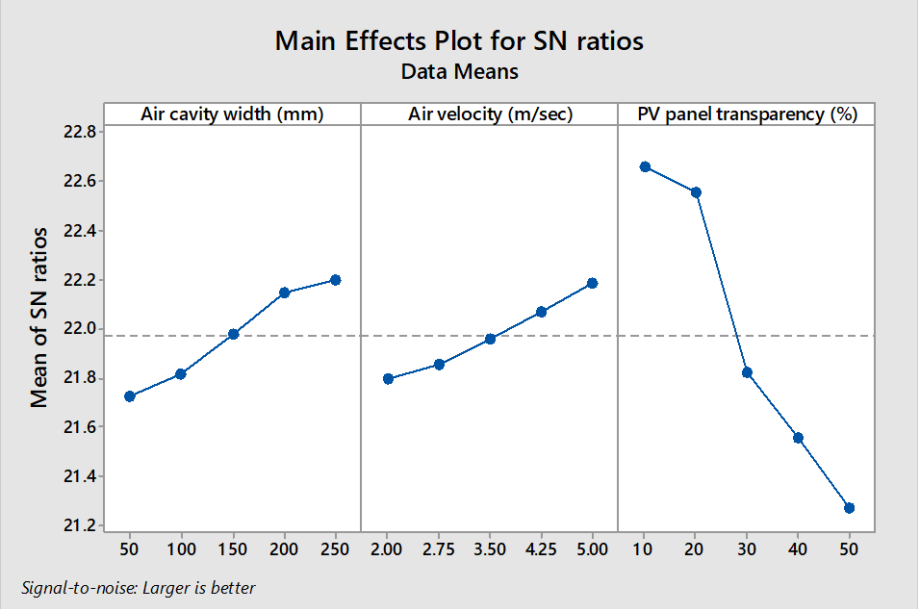

Figure 8. Impact of air cavity, air velocity and transparency of PV panel on power of PV panel.

Figure 8b illustrates how changes in air velocity affect the electrical power output of the photovoltaic (PV) panel. An increase in air velocity enhances the rate of heat dissipation from the panel, resulting in an upward trend in power output, as reflected by the rising signal-to-noise (S/N) ratio. This relationship indicates that higher air velocities contribute to improved thermal management of the PV panel, thereby boosting its efficiency. Enhanced air movement helps to dissipate heat more effectively, preventing the panel from overheating and maintaining optimal operating temperatures, which in turn maximises the electrical output of the PV panel. Similar observations have been reported by Preet et al. [19].

Figure 8c depicts the impact of varying transparency levels on the power output of the photovoltaic (PV) panel. The results show a significant decrease in power output as the transparency of the panel increases. This decline is primarily due to the reduced area covered by photovoltaic cells, which leads to lower energy conversion efficiency. These findings are consistent with the research conducted by Miyazaki et al. [11], which similarly highlighted the trade-off between panel transparency and power output. As transparency increases, more light passes through the panel without being converted into electricity, thus reducing the overall power output.

c) Main effect plot of daylight illuminance in built space

Figure 9a illustrates the main effect plot for daylight illuminance in the built environment at different air cavity thicknesses. The results indicate a consistent decline in illuminance, as reflected by a decreasing signal-to-noise (S/N) ratio with increasing cavity thickness. This reduction is attributed to the growing number of

daylight reference points between the exterior and interior spaces, which impedes natural light penetration. These findings align with previous research conducted by Peng et al. [65] and Ioannidis et al. [67], which also observed that increased cavity thickness can obstruct natural light, reducing overall daylight illuminance within the built environment.

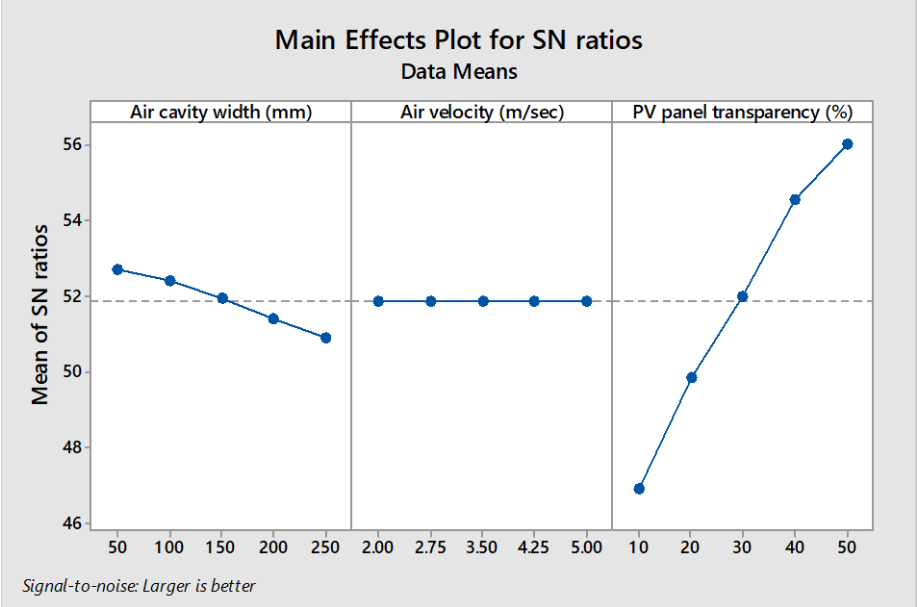

Figure 9. Impact of air cavity, air velocity and transparency of PV panel on daylight illuminance.

In contrast, **Figure 9b** shows that changes in air velocity have no impact on indoor illuminance, with the signal-to-noise (S/N) ratio remaining constant. **Figure 9c** demonstrates a significant improvement in daylight illuminance as the transparency of the photovoltaic panel increases, indicated by a rise in the S/N ratio. This enhancement is due to the larger clear surface area associated with higher panel transparency, which facilitates greater light transmission into the built space. Similar observations were made by Miyazaki et al. [11], confirming the beneficial effects of panel transparency on natural lighting.

5.2. Mathematical correlations

The regression analysis technique is applied to create mathematical relationships for the Solar Heat Gain Coefficient (SHGC), photovoltaic panel power output, and daylight illuminance within the built environment. The design parameters are regressed against the SHGC, power output, and illuminance values obtained from experimental runs, which were conducted using the Taguchi method in a hot composite climate zone, as detailed in **Table 2**. These mathematical models are derived from the experimental response data. This multiple linear regression approach converts the responses into mathematical expressions, as follows:

$$\mathrm{SHGC}_{\mathrm{computed}} = 0.18381 - 0.000117\ \text{Air cavity (mm)} + 0.00557\ \text{Air velocity (m/s)} + 0.001256\ \text{Transparency (\%)} \quad (5)$$

$$\text{Power}_{\text{computed}}\ (\text{W}) = 12.981 + 0.003724\ \text{Air cavity (mm)} + 0.1941\ \text{Air velocity (m/s)} - 0.05468\ \text{Transparency (\%)} \quad (6)$$

$$\text{Daylight illuminance}_{\text{computed}}\ (\text{Lux}) = 162.9 - 0.4240\ \text{Air cavity (mm)} + 10.466\ \text{Transparency (\%)} \quad (7)$$

Equation (5) demonstrates that air cavity thickness negatively impacts the Solar Heat Gain Coefficient (SHGC), whereas both air velocity and the transparency of the photovoltaic panel have a positive effect. Similarly, Equation (6) shows that air velocity and cavity thickness boost the power output of the photovoltaic panel, while panel transparency reduces it. Conversely, Equation (7) indicates that cavity thickness negatively affects daylight illuminance, while greater transparency of the photovoltaic panel enhances it. As previously mentioned, air velocity does not influence indoor illuminance. This approach is consistent with the methodologies used by several researchers, including Vyas et al. [56], Tewari et al. [57], Kumar et al. [54], Sharma et al. [47] and Preet et al. [39], who have also utilised multiple linear regression (MLR) techniques to develop mathematical correlations based on experimental data.

5.3. Validations of mathematical correlations

This section discusses the validation of the mathematical correlations for the responses using the ANOVA (Analysis of Variance) method. The credibility of these mathematical correlations has been confirmed through experimental investigations, ensuring their reliability and accuracy in predicting the performance metrics of the mechanically ventilated photovoltaic-DSF system.

5.3.1. Statistical validation

To evaluate the statistical significance of the design parameters on the responses, ANOVA (Analysis of Variance) was performed on the output obtained for each response. This method estimates the impact of each design parameter, thereby contributing to the robustness of the findings [68]. The *F*-test assesses the effects of different design parameters on the responses, providing a *p*-value for each *F*-value that indicates the significance of a particular design parameter. This analysis was conducted at a 5% significance level, corresponding to a 95% confidence level [59]. Generally, a *p*-value below 0.05 suggests a substantial contribution from the specified parameter, while a higher *p*-value indicates minimal contribution [54].

Table 5 illustrates the statistical significance of the design parameters concerning SHGC (Solar Heat Gain Coefficient), the power output of the photovoltaic panel, and daylight illuminance correlations. The results reveal that all three design parameters significantly influence both SHGC and photovoltaic power, as their *p*-values are below 0.05. This low *p*-value indicates that the likelihood of the observed effects occurring by chance is very small, thus confirming the significance of the design parameters on SHGC and photovoltaic power output. However, the impact of air velocity on daylight illuminance is not significant. The signal-to-noise (S/N) ratio remains constant, indicating that changes in air velocity do not affect daylight illuminance. Consequently, the *p*-value for air velocity exceeds 0.05, suggesting that any observed differences in daylight illuminance due to air velocity are likely due to chance, and thus, air velocity does not have a statistically significant effect on daylight

illuminance. In summary, while the design parameters significantly influence SHGC and photovoltaic power output, air velocity does not significantly affect daylight illuminance.

The coefficient of determination (R^2) exceeds 0.9 for the correlations of all responses, indicating that the results are statistically significant [54,57]. This high R^2 value demonstrates that the model explains over 90% of the variability in the responses, underscoring the reliability of the findings. Additionally, the low *p*-values for SHGC and photovoltaic power output confirm that the design parameters have a significant effect on these responses, validating the experimental design and analysis approach. The statistical significance of these parameters ensures that the observed effects are not due to random variation but are indeed attributable to the changes in the design parameters.

Table 5. *p*-value of different design parameters on responses.

Parameters	Solar heat gain coefficient (SHGC)	Power of PV panel	Lux level
Air cavity	0.002	0.002	0.000
Air velocity	0.008	0.004	0.48
Transparency of PV panel	0.000	0.000	0.000

Figures 10a–**c** display scatter plots that compare the experimental values of SHGC, photovoltaic power, and illuminance with the values calculated from the mathematical models. Additionally, normal probability plots are used to evaluate the normality of the residuals, with data plotted against the theoretical normal distribution. It is crucial that the points form a line that is nearly straight; deviations from this linearity indicate a lack of normality [59]. The normal probability plots for SHGC, photovoltaic power, and daylight illuminance, shown in **Figure 11**, meet these criteria, confirming the adequacy of the developed mathematical correlations.

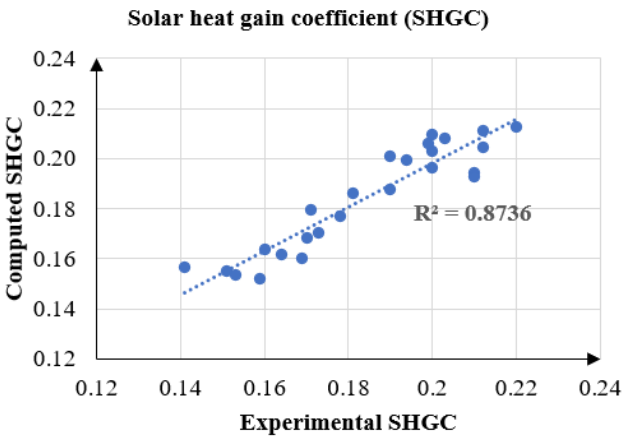

(**a**)

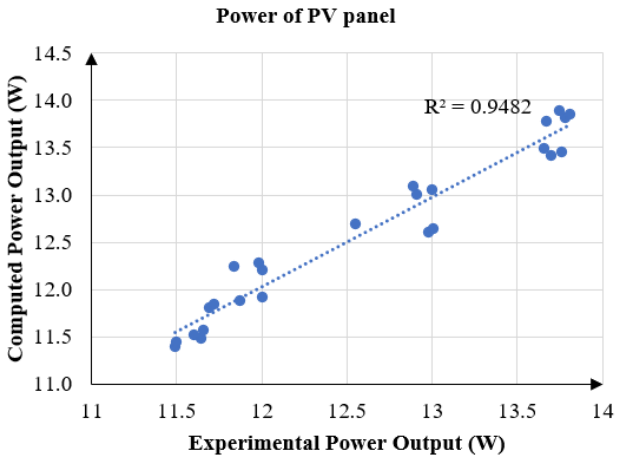

(**b**)

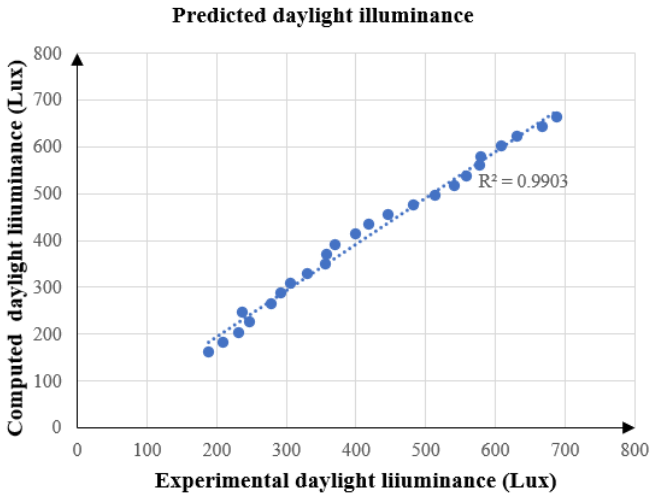

(**c**)

Figure 10. Curve fitting for **(a)** SHGC; **(b)** power of PV panel and **(c)** daylight illuminance.

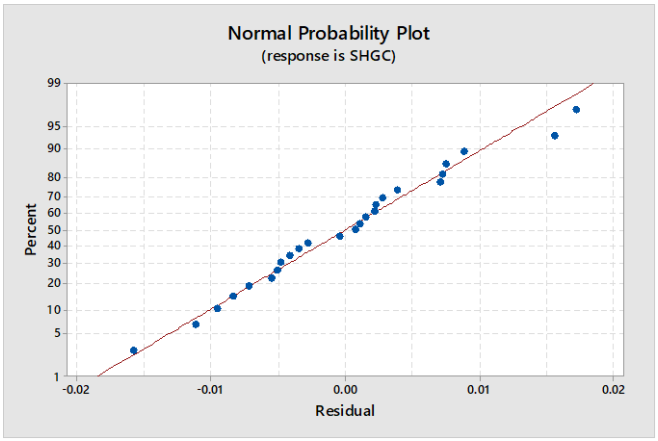

(**a**)

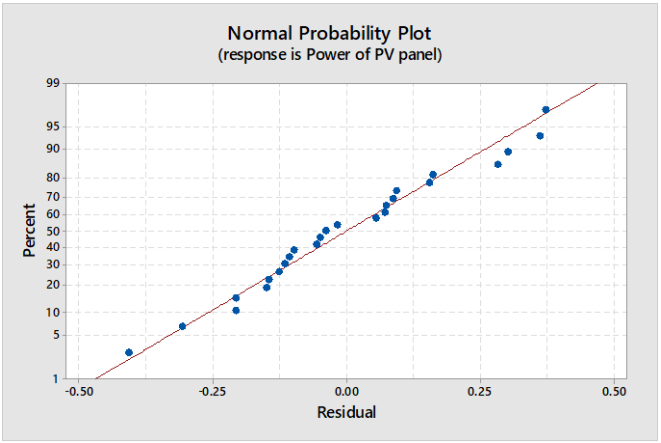

(**b**)

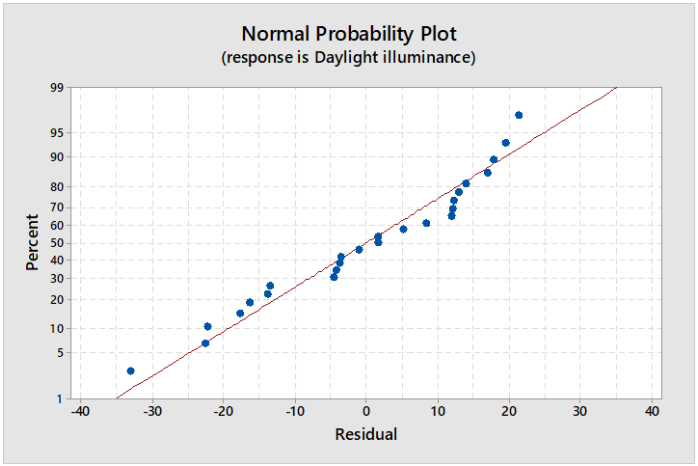

(**c**)

Figure 11. Normal probability plot for **(a)** SHGC; **(b)** power of PV panel and **(c)** Daylight illuminance.

5.3.2. Field validation

Further experiments were carried out using both optimal and random settings of the design parameters to validate the robustness of the developed mathematical

correlations. These validation experiments were conducted under the same experimental setup during the cold climatic conditions of the composite climate zone. **Table 6** presents the results obtained from both optimal and random parameter configurations. The findings indicate that the proposed model's adequacy falls within an acceptable range, with the relative error being within 5%. The analysis reveals that the transparency of the photovoltaic panel had the most significant impact on the Solar Heat Gain Coefficient (SHGC), the electrical power output of the photovoltaic panel, and daylight illuminance within the built environment under cold climatic conditions.

Table 6. Results of the model equation output against the experimental output.

	Air cavity (mm)	Air velocity (m/s)	Transparency of PV panel (%)	Experimental	Model equation	Error (%)
SHGC (optimum)	50	5	50	0.219	0.230	4.78
SHGC (random)	150	3.5	10	0.152	0.159	4.44
Power of PV panel (optimum)	250	5	10	13.72	14.335	4.29
Power of PV panel (random)	150	4.25	50	12.44	12.98	4.16
Daylight illuminance (optimum)	50		50	639	665	3.91
Daylight illuminance (random)	150		10	196	203	3.44

5.4. Uncertainty analysis

On the behalf of the sensitivity and accuracy of the measuring instruments used in present investigation, the uncertainty of the solar heat gain was conducted [47]. The Uncertainty of the solar heat gain coefficient is calculated as follows:

$$SHGC_{error} = \pm\left(\left|\left(\frac{G_1}{G_1+G_2+G_3}\right)\gamma_{G_1} + \left(\frac{G_2}{G_1+G_2+G_3}\right)\gamma_{G_2} + \left(\frac{G_3}{G_1+G_2+G_3}\right)\gamma_{G_3}\right| - \left|\frac{2}{G_4}\right|\right) \quad (8)$$

In the above equation, γ_{G_1}, γ_{G_2} and γ_{G_3} are relative errors of G1, G2 and G3, respectively. The values of the γ_{G_1}, γ_{G_2} and γ_{G_3} are taken to be 0.2%, 3% and 3%, respectively. In experimental case number 7, the convective heat flux and radiative heat flux were observed to be 42 W/m^2 and 54 W/m^2, respectively. The indoor radiation was found to be 62 W/m^2, while the solar radiation incident on the outer skin of the system was measured at 747 W/m^2. The Solar Heat Gain Coefficient (SHGC) was calculated to be 0.210, with an uncertainty of approximately ±2.4%.

6. Conclusion

This study aims to optimise the design parameters of mechanically ventilated photovoltaic-double skin façade (PV-DSF) systems for winter conditions in India's composite climate. By utilising the Taguchi L25 orthogonal array and multiple linear regression techniques, the research establishes mathematical correlations to predict the Solar Heat Gain Coefficient (SHGC), daylight illuminance, and power output of photovoltaic panels. These correlations are then applied to evaluate the energy performance and savings of the mechanical ventilated PV-DSF system during cold

weather in the Indian composite environment, assessing its effectiveness in improving energy efficiency.

Key conclusions from the research include:

- The developed mathematical correlations have accurately estimated the thermal and electrical performance of the mechanical ventilated PV-DSF system during winter. Validation through ANOVA confirmed the statistical significance of the relationships between design parameters and responses, ensuring the robustness and reliability of these correlations for precisely predicting the system's energy behaviour in winter conditions.
- A strong correlation ($R^2 > 0.90$) exists between the experimental results and values calculated using the developed mathematical models. This high R^2 value indicates that the proposed correlations accurately predict the system's performance, capturing over 90% of the variability in the experimental data.
- An optimal design combination for maximising energy performance in cold climatic conditions includes a mechanically ventilated PV-DSF system with a photovoltaic panel that has 50% transparency, an air velocity of 5 m/s, and a 50 mm air cavity. This configuration effectively balances thermal and electrical performance.

The experimental findings show that air cavity thickness, air velocity, and photovoltaic panel transparency significantly impact the energy performance of mechanical ventilated PV-DSF systems. The insights gained from this study help identify the optimal combination of these parameters, maximising energy savings in the cold climatic conditions of the composite climate zone. Such optimisation can enhance both thermal and electrical performance in these environments.

Based on the findings of this study, we recommend several areas for future research to further enhance the understanding and application of mechanically ventilated photovoltaic-double skin façade (PV-DSF) systems in India's composite climate during winter conditions:

- Exploring the impact of additional variables, such as different climatic conditions, slat angle and position of venetian blinds, building orientations, and material properties, could provide a more comprehensive understanding of the factors influencing the energy performance of mechanical ventilated PV-DSF system.
- Conducting a comprehensive techno-economic analysis of the mechanical ventilated PV-DSF system will provide valuable insights into its cost-effectiveness and economic viability. This analysis should consider initial installation costs, maintenance expenses, and potential energy savings over the system's lifespan.
- Performing a life cycle assessment will help evaluate the environmental impact of the mechanical PV-DSF system from production to disposal. This assessment can identify areas for improvement in sustainability and guide the development of more eco-friendly design options.
- Future studies should include a broader range of data points and longer observation periods to validate the findings across different conditions and settings. This will help in generalizing the results and improving their reliability.

- Incorporating advanced statistical and machine learning models could provide deeper insights into the complex interactions between design parameters. These techniques can help identify non-linear relationships and potential synergies that were not captured in the current study.
- Future research should also consider the sustainability and cost implications of the design parameters. Analyzing the trade-offs between energy efficiency, environmental impact, and economic feasibility will provide a holistic view of the benefits and challenges associated with different design choices.

By addressing these areas, future research can build on the current study's findings and contribute to the development of more efficient and sustainable building designs. These recommendations aim to enhance both the thermal and electrical performance of PV-DSF systems, maximizing energy savings in the cold climatic conditions of the composite climate zone.

Author contributions: Conceptualization, SP, SM and JM; methodology, SP and HS; software, SP and HS; validation, SP and STS; formal analysis, SP; investigation, SP; resources, SM and JM; data curation, SP; writing—original draft preparation, SP; writing—review and editing, SM and STS; visualization, STS; supervision, SM and JM; project administration, SM; funding acquisition, SM. All authors have read and agreed to the published version of the manuscript.

Funding: This work is supported by a DST project named "Development and performance analysis of Semi-Transparent Solar Photovoltaic double pane Window/Facade system" funded by the Department of Science and Technology, Government of India (TMD/CERI/BEE/2016/070(G).

Institutional review board statement: Not applicable.

Informed consent statement: Not applicable.

Data availability statement: The authors confirm that the data obtained and analysed during the findings of this research work are available within the article.

Conflict of interest: The authors declare no conflict of interest.

Nomenclature

SHGC	Solar heat gain coefficient
DSF	Double skin façade
PV	Photovoltaic panel
PV-DSF	Photovoltaic-double skin facade
ANOVA	Analysis of variance
S/N ratio	Signal to noise ratio

References

1. Preet S, Smith ST. A comprehensive review on the recycling technology of silicon based photovoltaic solar panels: Challenges and future outlook. Journal of Cleaner Production. 2024; 448: 141661. doi: 10.1016/j.jclepro.2024.141661
2. Preet S, Bhushan B, Mahajan T. Experimental investigation of water based photovoltaic/thermal (PV/T) system with and without phase change material (PCM). Solar Energy. 2017; 155: 1104–1120. doi: 10.1016/j.solener.2017.07.040

3. Preet S, Mathur S, Mathur J, et al. Energy characterization of forced ventilated Photovoltaic-DSF system in hot summer of composite climate. Energy and Built Environment. 2024; 5(5): 704–718. doi: 10.1016/j.enbenv.2023.05.008
4. Saxena P, Das S. Analysis of Energy Saving Potential of a Residential Building Complex using Energy Conservation Building Code 2017. In: Proceedings of the 6th Annual International Conference on Architecture and Civil Engineering (ACE 2018); 14–15 May 2018; Singapore.
5. Chen X, Yang H. A multi-stage optimization of passively designed high-rise residential buildings in multiple building operation scenarios. Applied Energy. 2017; 206: 541–557. doi: 10.1016/j.apenergy.2017.08.204
6. Yao R, Costanzo V, Li X, et al. The effect of passive measures on thermal comfort and energy conservation. A case study of the hot summer and cold winter climate in the Yangtze River region. Journal of Building Engineering. 2018; 15: 298–310. doi: 10.1016/j.jobe.2017.11.012
7. Pomponi F, Piroozfar PAE, Southall R, et al. Energy performance of Double-Skin Façades in temperate climates: A systematic review and meta-analysis. Renewable and Sustainable Energy Reviews. 2016; 54: 1525–1536. doi: 10.1016/j.rser.2015.10.075
8. Kim D, Cox SJ, Cho H, et al. Comparative investigation on building energy performance of double skin façade (DSF) with interior or exterior slat blinds. Journal of Building Engineering. 2018; 20: 411–423. doi: 10.1016/j.jobe.2018.08.012
9. Agathokleous RA, Kalogirou SA. Double skin facades (DSF) and building integrated photovoltaics (BIPV): A review of configurations and heat transfer characteristics. Renewable Energy. 2016; 89: 743–756. doi: 10.1016/j.renene.2015.12.043
10. Lu L, Law KM. Overall energy performance of semi-transparent single-glazed photovoltaic (PV) window for a typical office in Hong Kong. Renewable Energy. 2013; 49: 250–254. doi: 10.1016/j.renene.2012.01.021
11. Miyazaki T, Akisawa A, Kashiwagi T. Energy savings of office buildings by the use of semi-transparent solar cells for windows. Renewable Energy. 2005; 30(3): 281–304. doi: 10.1016/j.renene.2004.05.010
12. Wang M, Peng J, Li N, et al. Comparison of energy performance between PV double skin facades and PV insulating glass units. Applied Energy. 2017; 194: 148–160. doi: 10.1016/j.apenergy.2017.03.019
13. Chen M, Zhang W, Xie L, et al. Experimental and numerical evaluation of the crystalline silicon PV window under the climatic conditions in southwest China. Energy. 2019; 183: 584–598. doi: 10.1016/j.energy.2019.06.146
14. Wang C, Ji J, Uddin MM, et al. The study of a double-skin ventilated window integrated with CdTe cells in a rural building. Energy. 2021; 215: 119043. doi: 10.1016/j.energy.2020.119043
15. Preet S. A review on the outlook of thermal management of photovoltaic panel using phase change material. Energy and Climate Change. 2021; 2: 100033. doi: 10.1016/j.egycc.2021.100033
16. Ioannidis Z, Rounis ED, Athienitis A, et al. Double skin façade integrating semi-transparent photovoltaics: Experimental study on forced convection and heat recovery. Applied Energy. 2020; 278: 115647. doi: 10.1016/j.apenergy.2020.115647
17. Radmard H, Ghadamian H, Esmailie F, et al. Examining a numerical model validity for performance evaluation of a prototype solar oriented Double skin Façade: Estimating the technical potential for energy saving. Solar Energy. 2020; 211: 799–809. doi: 10.1016/j.solener.2020.10.017
18. Yang S, Cannavale A, Di Carlo A, et al. Performance assessment of BIPV/T double-skin façade for various climate zones in Australia: Effects on energy consumption. Solar Energy. 2020; 199: 377–399. doi: 10.1016/j.solener.2020.02.044
19. Preet S, Sharma MK, Mathur J, et al. Performance evaluation of photovoltaic double-skin facade with forced ventilation in the composite climate. Journal of Building Engineering. 2020; 32: 101733. doi: 10.1016/j.jobe.2020.101733
20. Barbosa S, Ip K, Southall R. Thermal comfort in naturally ventilated buildings with double skin façade under tropical climate conditions: The influence of key design parameters. Energy and Buildings. 2015; 109: 397–406. doi: 10.1016/j.enbuild.2015.10.029
21. Preet S, Mathur J, Mathur S. Influence of geometric design parameters of double skin façade on its thermal and fluid dynamics behavior: A comprehensive review. Solar Energy. 2022; 236: 249–279. doi: 10.1016/j.solener.2022.02.055
22. Jankovic A, Siddiqui MS, Goia F. Laboratory testbed and methods for flexible characterization of thermal and fluid dynamic behaviour of double skin facades. Building and Environment. 2022; 210: 108700. doi: 10.1016/j.buildenv.2021.108700
23. Peng J, Lu L, Yang H, et al. Comparative study of the thermal and power performances of a semi-transparent photovoltaic façade under different ventilation modes. Applied Energy. 2015; 138: 572–583. doi: 10.1016/j.apenergy.2014.10.003
24. Wang Y, Chen Y, Li C. Energy performance and applicability of naturally ventilated double skin façade with Venetian blinds in Yangtze River Area. Sustainable Cities and Society. 2020; 61: 102348. doi: 10.1016/j.scs.2020.102348

25. Srisamranrungruang T, Hiyama K. Balancing of natural ventilation, daylight, thermal effect for a building with double-skin perforated facade (DSPF). Energy and Buildings. 2020; 210: 109765. doi: 10.1016/j.enbuild.2020.109765
26. Sharma MK, Preet S, Mathur J, et al. Exploring the advantages of photo-voltaic triple skin façade in hot summer conditions. Solar Energy. 2021; 217: 317–327. doi: 10.1016/j.solener.2021.02.020
27. Zhang Y, Zhang Y, Li Z. A novel productive double skin façades for residential buildings: Concept, design and daylighting performance investigation. Building and Environment. 2022; 212: 108817. doi: 10.1016/j.buildenv.2022.108817
28. Han J, Lu L, Peng J, et al. Performance of ventilated double-sided PV façade compared with conventional clear glass façade. Energy and Buildings. 2013; 56: 204–209. doi: 10.1016/j.enbuild.2012.08.017
29. Peng J, Lu L, Yang H. An experimental study of the thermal performance of a novel photovoltaic double-skin facade in Hong Kong. Solar Energy. 2013; 97: 293–304. doi: 10.1016/j.solener.2013.08.031
30. Inan T, Basaran T. Experimental and numerical investigation of forced convection in a double skin façade by using nodal network approach for Istanbul. Solar Energy. 2019; 183: 441–452. doi: 10.1016/j.solener.2019.03.030
31. Pourshab N, Tehrani MD, Toghraie D, et al. Application of double glazed façades with horizontal and vertical louvers to increase natural air flow in office buildings. Energy. 2020; 200: 117486. doi: 10.1016/j.energy.2020.117486
32. Jankovic A, Goia F. Characterization of a naturally ventilated double-skin façade through the design of experiments (DOE) methodology in a controlled environment. Energy and Buildings. 2022; 263: 112024. doi: 10.1016/j.enbuild.2022.112024
33. Tao Y, Yan Y, Fang X, et al. Solar-assisted naturally ventilated double skin façade for buildings: Room impacts and indoor air quality. Building and Environment. 2022; 216: 109002. doi: 10.1016/j.buildenv.2022.109002
34. Lin Z, Song Y, Chu Y. Summer performance of a naturally ventilated double-skin facade with adjustable glazed louvers for building energy retrofitting. Energy and Buildings. 2022; 267: 112163. doi: 10.1016/j.enbuild.2022.112163
35. Jankovic A, Goia F. Control of heat transfer in single-story mechanically ventilated double skin facades. Energy and Buildings. 2022; 271: 112304. doi: 10.1016/j.enbuild.2022.112304
36. Tao Y, Fang X, Setunge S, et al. Naturally ventilated double-skin façade with adjustable louvers. Solar Energy. 2021; 225: 33–43. doi: 10.1016/j.solener.2021.07.013
37. Sotelo-Salas C, Escobar-del Pozo C, Esparza-López CJ. Thermal assessment of spray evaporative cooling in opaque double skin facade for cooling load reduction in hot arid climate. Journal of Building Engineering. 2021; 38: 102156. doi: 10.1016/j.jobe.2021.102156
38. Tao Y, Zhang H, Huang D, et al. Ventilation performance of a naturally ventilated double skin façade with low-e glazing. Energy. 2021; 229: 120706. doi: 10.1016/j.energy.2021.120706
39. Preet S, Mathur S, Mathur J, et al. Development of mathematical correlations to predict performance of forced ventilated Photovoltaic-DSF system in hot composite climate. Journal of Building Physics. 2024; 48(1): 31–66. doi: 10.1177/17442591241247327
40. Bansal NK, Minke G. In: Climatic zones and rural housing in India. Forschungszentrum Jülich GmbH, Zentralbibliothek; 1995.
41. Kumar S, Mathur J, Mathur S, et al. An adaptive approach to define thermal comfort zones on psychrometric chart for naturally ventilated buildings in composite climate of India. Building and Environment. 2016; 109: 135–153. doi: 10.1016/j.buildenv.2016.09.023.
42. Agarwal P, Prabhakar A. Energy and thermo-economic analysis of PCM integrated brick in composite climatic condition of Jaipur - A numerical study. Sustainable Cities and Society. 2023; 88: 104294. doi: 10.1016/j.scs.2022.104294
43. Kumar S, Singh MK, Mathur A, et al. Thermal performance and comfort potential estimation in low-rise high thermal mass naturally ventilated office buildings in India: An experimental study. Journal of Building Engineering. 2018; 20: 569–584. doi: 10.1016/j.jobe.2018.09.003
44. National Fenestration Rating Council. In: NFRC 201–2014 Procedure for Interim Standard Test Method for Measuring the Solar Heat Gain Coefficient of Fenestration Systems Using Calorimetry Hot Box Methods. National Fenestration Rating Council; 2014.
45. Zarei A, Liravi M, Rabiee MB, et al. A Novel, eco-friendly combined solar cooling and heating system, powered by hybrid Photovoltaic thermal (PVT) collector for domestic application. Energy Conversion and Management. 2020; 222: 113198. doi: 10.1016/j.enconman.2020.113198
46. Wu JH, Yang LD, Hou J. Experimental performance study of a small wall room air conditioner retrofitted with R290 and R1270. International Journal of Refrigeration. 2012; 35(7): 1860–1868. doi: 10.1016/j.ijrefrig.2012.06.004

47. Sharma MK, Preet S, Mathur J, et al. Parametric analysis of factors affecting thermal performance of photovoltaic triple skin façade system (PV-TSF). Journal of Building Engineering. 2021; 40: 102344. doi: 10.1016/j.jobe.2021.102344
48. Sukhatme K, Sukhatme SP. In: Solar energy: principles of thermal collection and storage. Tata McGraw-Hill; 1996.
49. Ravuri M, Reddy YSK, Vardhan DH. Parametric optimization of face turning parameters for surface roughness on EN 31 material using RSM and Taguchi method. Materials Today: Proceedings. 2021; 37: 769–774. doi: 10.1016/j.matpr.2020.05.816
50. Gul M, Kalam MA, Mujtaba MA, et al. Multi-objective-optimization of process parameters of industrial-gas-turbine fueled with natural gas by using Grey-Taguchi and ANN methods for better performance. Energy Reports. 2020; 6: 2394–2402. doi: 10.1016/j.egyr.2020.08.002
51. Sasmito AP, Kurnia JC, Shamim T, et al. Optimization of an open-cathode polymer electrolyte fuel cells stack utilizing Taguchi method. Applied Energy. 2017; 185: 1225–1232. doi: 10.1016/j.apenergy.2015.12.098
52. Varun, Patnaik A, Saini RP, et al. Performance prediction of solar air heater having roughened duct provided with transverse and inclined ribs as artificial roughness. Renewable Energy. 2009; 34(12): 2914–2922. doi: 10.1016/j.renene.2009.04.030
53. Roy RK. In: A primer on the Taguchi method. Society of Manufacturing Engineers; 2010.
54. Kumar S, Tewari P, Mathur S, et al. Development of mathematical correlations for indoor temperature from field observations of the performance of high thermal mass buildings in India. Building and Environment. 2017; 122: 324–342. doi: 10.1016/j.buildenv.2017.06.030
55. Türkmen İ, Gül R, Çelik C. A Taguchi approach for investigation of some physical properties of concrete produced from mineral admixtures. Building and Environment. 2008; 43(6): 1127–1137. doi: 10.1016/j.buildenv.2007.02.005
56. Vyas M, Jain M, Pareek K, et al. Multivariate optimization for maximum capacity of lead acid battery through Taguchi method. Measurement. 2019; 148: 106904. doi: 10.1016/j.measurement.2019.106904
57. Tewari P, Mathur S, Mathur J. Thermal performance prediction of office buildings using direct evaporative cooling systems in the composite climate of India. Building and Environment. 2019; 157: 64–78. doi: 10.1016/j.buildenv.2019.04.044
58. Dehnad K. In: Quality control, robust design, and the Taguchi method. Springer Science & Business Media; 2012.
59. Sinha R, Mathur S. Use of activated silica sol as a coagulant aid to remove aluminium from water defluoridated by electrocoagulation. Desalination and Water Treatment. 2016; 57(36): 16790–16799. doi: 10.1080/19443994.2015.1084536
60. Yi H, Srinivasan RS, Braham WW. An integrated energy—emergy approach to building form optimization: Use of EnergyPlus, emergy analysis and Taguchi-regression method. Building and Environment. 2015; 84: 89–104. doi: 10.1016/j.buildenv.2014.10.013
61. Mamourian M, Shirvan KM, Ellahi R, et al. Optimization of mixed convection heat transfer with entropy generation in a wavy surface square lid-driven cavity by means of Taguchi approach. International Journal of Heat and Mass Transfer. 2016; 102: 544–554. doi: 10.1016/j.ijheatmasstransfer.2016.06.056
62. Mathur J, Bansal NK, Mathur S, et al. Experimental investigations on solar chimney for room ventilation. Solar Energy. 2006; 80(8): 927–935. doi: 10.1016/j.solener.2005.08.008
63. Bhatnagar M, Mathur J, Garg V. Development of reference building models for India. Journal of Building Engineering. 2019; 21: 267–277. doi: 10.1016/j.jobe.2018.10.027
64. Preet S, Sharma MK, Mathur J, et al. Analytical model of semi-transparent photovoltaic double-skin façade system (STPV-DSF) for natural and forced ventilation modes. International Journal of Ventilation. 2021; 22(2): 138–167. doi: 10.1080/14733315.2021.1971873
65. Peng J, Curcija DC, Lu L, et al. Numerical investigation of the energy saving potential of a semi-transparent photovoltaic double-skin facade in a cool-summer Mediterranean climate. Applied Energy. 2016; 165: 345–356. doi: 10.1016/j.apenergy.2015.12.074
66. Mateus NM, Pinto A, da Graça GC. Validation of EnergyPlus thermal simulation of a double skin naturally and mechanically ventilated test cell. Energy and Buildings. 2014; 75: 511–522. doi: 10.1016/j.enbuild.2014.02.043
67. Ioannidis Z, Buonomano A, Athienitis AK, et al. Modeling of double skin façades integrating photovoltaic panels and automated roller shades: Analysis of the thermal and electrical performance. Energy and Buildings. 2017; 154: 618–632. doi: 10.1016/j.enbuild.2017.08.046
68. Faraway JJ. In: Practical regression and ANOVA using R. University of Bath; 2002.